MAGE-A4 pMHC-targeted CAR-T cells exploiting TCR machinery exhibit significantly improved in vivo function while retaining antigen specificity

Meiou Liu [ID],[1] Yasushi Akahori [ID],[1] Naoko Imai [ID],[1] Linan Wang [ID],[2] Kohei Negishi [ID],[1] Takuma Kato [ID],[3] Hiroshi Fujiwara [ID],[1] Hiroshi Miwa [ID],[1] Hiroshi Shiku,[1] Yoshihiro Miyahara [ID] [1]

[1]Personalized Cancer Immunotherapy, Mie University Graduate School of Medicine, Tsu, Japan
[2]Hematology and Oncology, Mie University Graduate School of Medicine, Tsu, Japan
[3]Immunology, Nagoya University Graduate School of Medicine, Nagoya, Japan

Correspondence to
Dr Yoshihiro Miyahara;
miyahr-y@med.mie-u.ac.jp

ABSTRACT

Background The development of chimeric antigen receptor (CAR)-T cell therapies for solid tumors has attracted considerable attention, yet their clinical efficacy remains limited. Therefore, various efforts have been made to improve the efficacy of CAR-T cell therapy. As one promising strategy, incorporating the T-cell receptor (TCR) machinery into CAR structures has been reported to improve the efficacy of CAR-T cells in studies using conventional CARs targeting such as EGFR. However, in the case of peptide/major histocompatibility complex (pMHC)-targeted CARs, the advantages of exploiting TCR machinery have not been fully elucidated. We recently developed MAGE-A4-derived pMHC (MAGE-A4 pMHC)-targeted CAR-T cells (MA-CAR-T cells) using a highly specific human scFv antibody against MAGE-A4$_{p230-239}$/HLA-A*02:01. We aimed to determine whether MAGE-A4 pMHC-targeted CAR-T cells using the TCR machinery (Hybrid MA-TCR-T cells) exhibit superior functionality without compromising antigen specificity.

Methods We constructed a retroviral vector expressing Hybrid MA-TCR where MAGE-A4 pMHC-specific scFv are fused to human TCR constant chains.

Results Hybrid MA-TCR-T cells demonstrated superior in vitro functions compared with MA-CAR-T cells, while maintaining strict antigen specificity. In addition, functional superiority of Hybrid MA-TCR-T cells to MA-CAR-T cells became more pronounced on repetitive antigen stimulation. In particular, Hybrid MA-TCR-T cells significantly inhibited tumor growth in an immunodeficient mouse model more effectively than MA-CAR-T cells. Ex vivo analyses indicated that their enhanced therapeutic efficacy might result from higher infiltration of functionally active, less differentiated Hybrid MA-TCR-T cells in tumor tissues.

Conclusions These findings suggest that leveraging the TCR machinery is a promising strategy for enhancing pMHC-targeted CAR-T cell therapy for solid tumors, potentially leading to more effective treatments.

INTRODUCTION

The clinical efficacy of chimeric antigen receptor (CAR)-T cell therapies has revolutionized the treatment of patients with

WHAT IS ALREADY KNOWN ON THIS TOPIC

⇒ Exploitation of T-cell receptor (TCR) machinery by conventional chimeric antigen receptors (CARs) targeting cell surface molecules, such as CD19 and EGFR, improves in vitro and in vivo functions of CAR-T cells.

WHAT THIS STUDY ADDS

⇒ MAGE-A4$_{p230-239}$/HLA-A*02:01-targeted CAR-T cells exploiting TCR machinery exhibit significantly enhanced in vitro and in vivo functionalities without compromising antigen specificity.

HOW THIS STUDY MIGHT AFFECT RESEARCH, PRACTICE OR POLICY

⇒ The results obtained in this study indicate that the strategy of exploiting TCR machinery could improve efficacies of peptide-major histocompatibility complex-targeted CAR-T cells, potentially leading to the development of more effective CAR-T therapies for solid tumors.

hematological malignancies, paving the way for their potential use in solid tumors.[1 2] However, their success in solid tumors remains limited,[3 4] with a few promising therapies targeting disialoganglioside GD2, Claudin-6, and Claudin-18.2.[5–7] A major challenge is the scarcity of tumor-specific cell surface molecules, which are ideal targets for CAR-T therapy.

One strategy to overcome this barrier involves the development of CARs that use the scFv antibody, which recognizes the peptide-major histocompatibility complex class I (pMHC), to target a variety of intracellular tumor-specific antigens.[8–10] Our group recently reported a novel pMHC-targeted CAR-T cell therapy using a highly specific human scFv antibody against MAGE-A4$_{p230-239}$/HLA-A*02:01 (MA-CAR-T).[11]

However, the broader application of CAR-T therapy for solid tumors is hindered by the low in vivo functionality of CAR-T cells, as evidenced by the overall lack of efficacy across various CAR-T therapies for solid tumors.[12 13] The primary factors contributing to this low efficacy include the unique structure of solid tumors, which necessitates efficient CAR-T cell trafficking to tumor sites and the immunosuppressive tumor microenvironment (TME). Additionally, intrinsic functional defects of CAR-T cells, such as exhaustion due to tonic signaling in either a ligand-dependent or ligand-independent manner, result in low persistency and hypo-responsiveness.[14–17] Therefore, various technological innovations have been made to CAR constructs to enhance CAR-T cell trafficking into solid tumors, confer resistance against inhibitory signals in the TME, and improve in vivo persistence by reducing tonic signaling and/or altering the TME milieu.[18–20]

Among these advances, several groups have recently reported novel CAR constructs, including AbTCR,[21] TAC,[22] TRuC,[23] STAR,[24] and HIT.[25] These constructs share the strategy of incorporating TCR machinery into CAR structures. These studies indicate that CAR-T cells exploiting TCR machinery enhanced in vitro and in vivo functions when conventional CARs targeting CD19 and EGFR are used as templates. Thus, incorporating TCR machinery into conventional CARs has potential for improving CAR-T functions and subsequent therapeutic outcomes in clinical settings.

However, the functional benefits of using TCR machinery in pMHC-targeted CARs remain unclear. Furthermore, detailed analyses of antigen specificity changes, which could potentially damage normal tissues, are lacking. Therefore, in this study, we performed a head-to-head comparative functional analysis to clarify the advantages of pMHC-targeted CAR-T exploiting TCR machinery (Hybrid MA-TCR-T) using a well-characterized MAGE-A4 pMHC-targeted CAR. Our results lay the foundation for pMHC-targeted CAR-T cell therapy for solid tumors.

METHODS
Cell lines
SK-MEL-37 and NW-MEL-38 are MAGE-A4$^+$/HLA-A*02:01$^+$ melanoma cell lines. The MAGE-A4$^-$/HLA-A*02:01$^+$ colon cancer cell line HCT116 served as a negative control. HLA-A*02:01$^+$ TAP-deficient T2 cells, which effectively load exogenous peptides, were used to stimulate MA-CAR-T or Hybrid MA-TCR-T cells. All cell lines were cultured in Roswell Park Memorial Institute (RPMI)-1640 medium (Thermo Fisher Scientific) supplemented with 10% fetal calf serum (Biowest), 2 mM glutamine, 100 U/mL penicillin, and 100 µg/mL streptomycin.

Peptides
MAGE-A4$_{p230-239}$ (GVYDGREHTV) and all peptides prepared for the cross-reactivity assay were synthesized at a purity higher than 80% (Invitrogen, Carlsbad, CA,

USA). All peptides were dissolved in dimethyl sulfoxide at a concentration of 10 mM and stored in aliquots at –80°C prior to use.

Vector construction and preparation of virus solutions
The construction of the MA-CAR expression vector has been previously described.[11] In summary, the monoclonal antibody scFv, highly specific to the MAGE-A4$_{p230-239}$/HLA-A*02:01 complex in the VH-VL orientation, along with a Cλ hinge domain, and a CD28 transmembrane domain containing CD3ζ and glucocorticoid-induced TNFR-related receptor (GITR) signaling domains, was inserted into a pMS3 retroviral vector (Takara Bio). For the Hybrid MA-TCR expressing vector, the identical monoclonal antibody scFv VL and VH were fused with the human TCR Cα and Cβ region, respectively. The two chains were linked by a furin-p2A cleavable peptide. TCR Cα and Cβ regions carried the following mutations: TCR-Cα T48C, TCR-Cβ S57C, and TCR-Cα transmembrane domain LSVIGFRIL mutated to LLVILLRIL.[26 27] This construct was inserted into the pMS3 retroviral vector. After transduction with the Lipofectamine LTX & PLUS reagent kit (Invitrogen) into Platinum-A packaging cells (Cell Biolabs), cell culture supernatants were used to produce virus solutions.

T cell transduction
Human T cells expressing MA-CAR or Hybrid MA-TCR were prepared by retroviral transduction, as previously described.[10 11] Briefly, peripheral blood mononuclear cells (PBMCs) were stimulated with plate-coated anti-CD3 (5 µg/mL; OKT3, Janssen Pharmaceutical, Beerse, Belgium) and RetroNectin (25 µg/mL; Takara Bio) on day 0. PBMCs were cultured in the GT-T551 medium (Takara Bio) supplemented with 300 IU/mL human recombinant IL-2 (Novartis), 0.2% human serum albumin (CLC Behring, USA), and 0.6% autologous human plasma. On days 3 and 4, these cells (mostly T cells) were transduced with the retroviral vector pMS3 containing MA-CAR or Hybrid MA-TCR using the RetroNectin-bound virus infection method. The retroviral solutions were preloaded onto RetroNectin (Takara Bio)-coated plates and centrifuged at 2000×g for 2 hours at 32°C, followed by expansion culture. The cells were used for experiments on days 10–14.

Antigen sensitivity assay and cross-reactivity assay
For antigen sensitivity assay, T2 cells were washed with plain RPMI medium and cultured in X-VIVO15 (Lonza) with MAGE-A4$_{p230-239}$ peptide at different concentrations for 18 hours. Then, T2 cells were rewashed with RPMI medium and cocultured with effector T cells for 24 hours. Subsequently, the supernatant was used to analyze interferon-gamma (IFN-γ) levels using a human IFN-γ ELISA development kit (Mabtech, USA) according to the manufacturer's instructions. In several experiments, we analyzed granzyme B or TNF-α levels using the human granzyme B or TNF-α ELISA development kit (Mabtech). For cross-reactivity analysis, the human IFN-γ levels were

detected using the ELISPOT assay. Effector cells (1×10^4) and peptide-pulsed T2 cells (1×10^4) were seeded into the anti-human IFN-γ monoclonal antibody (1-D1K; Mabtech) pre-coated plate. Following a 22-hour incubation at 37°C with 5% CO_2, the plate was washed, and the biotinylated anti-human IFN-γ monoclonal antibody (7-B6-1; Mabtech) was added. Subsequently, the plate was incubated at 4°C overnight. After washing plates, spots were developed using streptavidin-alkaline phosphatase conjugated (Roche) and Sigmafast BICP/NBT (Sigma-Aldrich). Spots were counted using an ELISPOT Plate Reader (ImmunoSpot, CTL-Europe).

Cellular cytotoxicity assay

For the T cell cytotoxicity assay, we used a non-radioactive cellular cytotoxicity assay kit (Techno Suzuta, Heiwa, Nagasaki, Japan), as previously described.[11 28] According to the manufacturer's instruction, 1×10^6/mL SK-MEL-37 cells or HCT116 cells were incubated with 2.5 µL of bis(butyryloxymethyl) 4′-hydroxymethyl-2,2′:6′,2″-terpyridine-6,6″-dicarboxylate (BM-HT) Reagent at 37°C and 5% CO_2 for 15 min. Subsequently, the cells were washed three times with RPMI1640, and 1×10^4/100 µL tumor cells per well were coculture with 100 µL effector cells at effector-to-target ratios of 10:1, 3:1, and 1:1 at 37°C with 5% CO_2. After coculturing for 120 min, the cells were centrifuged at 600×g for 5 min, and 25 µL of supernatant per well was mixed with 250 µL of europium solution. The 200 µL per well mixture was placed onto a 96-well White Polystyrene Plate (Thermo Fisher Scientific), and detection was performed using TriStar² S LB 942 Multimode Microplate Reader (Berthold Technologies). All experiments were performed in triplicates. Specific lysis (%) was calculated as 100×[experimental release (counts)−spontaneous release (counts)]/[maximum release (counts)−spontaneous release (counts)]. Long-term cytotoxicity was measured using the xCELLigence (ACEA Bioscience) impedance-based assay.[29] Briefly, tumor cells were plated at a density of 12,000 cells/well. After 17 hours, the effector cells were added to the wells at effector-to-target ratios of 5:1, 2:1, and 1:1. and tumor growth or death as indicated by cell index was monitored up to 80 hours.

Intracellular cytokine staining assay

For intracellular cytokine staining (ICS), effector cells (1×10^5 cells/well) were cocultured with tumor cells (1×10^5 cells/well) for 1 hour. A GolgiStop Protein Transport Inhibitor (BD Biosciences) was added, and the cells were incubated for an additional 4 hours. The final stimulus concentrations of phorbol 12-myristate 13-acetate and ionomycin are 50 nM and 1 µg/mL, respectively. Staining of cells for extracellular markers was performed, followed by fixation and permeabilization using a Cytofix/Cytoperm Kit (BD Biosciences) and subsequent IFN-γ staining.

Flow cytometry

Flow cytometry data for cell surface molecules and intracellular cytokines were collected using the LSR Fortessa X-20 (BD Bioscience) and analyzed with FlowJo software (FlowJo, Oregon). The following antibodies were used for cell surface and intracellular staining: PE/Cyanine7 anti-human CD8a (Clone: RPA-T8), PE/Cyanine7 anti-human CD4 (Clone: RPA-T4), APC anti-human CD4 (Clone: OKT-4), Brilliant Violet 421 anti-human CD45 (Clone: HI30), FITC anti-human CD45 (Clone: HI30), FITC anti-human CD62L (Clone: DREG-56), Brilliant Violet 711 anti-human CD45RA (Clone: HI100), APC anti-human CD279 (PD-1) (Clone: EH12.2H7), Brilliant Violet 711 anti-human CD366 (Tim-3) (Clone: F38-2E2), Brilliant Violet 421 anti-human CD223 (LAG-3) (Clone: 11C3C65), Brilliant Violet 421 anti-human CD69 (Clone: FN50), FITC anti-human CD25 (Clone: BC96), FITC Mouse IgG1, κ Isotype Ctrl (Clone: MOPC-21), APC Mouse IgG1, κ Isotype Ctrl (FC) (Clone: MOPC-21), Brilliant Violet 711 Mouse IgG1, κ Isotype Ctrl (Clone: MOPC-21), Brilliant Violet 421 Mouse IgG1, κ Isotype Ctrl (Clone: MOPC-21), Brilliant Violet 421 anti-human IFN-γ (Clone: 4S. B3). The antibodies were purchased from BioLegend. IFN-γ Monoclonal Antibody, eFluor 450 (Clone: 4S. B3) was purchased from eBiosciences (San Jose, CA, USA). MAGE-A4$^+$/HLA-A*02:01 PE-Tetramers were produced using refolded monomeric biotinylated pMHC and Streptavidin-R-Phycoerythrin (Agilent Technologies, Santa Clara, CA, USA) at a 1:4 molar ratio. Streptavidin-R-phycoerythrin was added in 10 aliquots, with 10 min of incubation at room temperature between each addition, then stored at 4°C.

Repetitive (chronic) antigen stimulation

24 well plates were coated with 10 µg/mL NeutrAvidin (Thermo Fisher Scientific) for 18 hours at 4°C. Then, plates were washed two times with PBS (−). Subsequently, the plates were coated with 10 µg/mL MAGE-A4$^+$/HLA-A*02:01 monomer for 18 hours at 4°C. On day 0, the plates were washed two times with PBS (−), then 5×10^5 MA-CAR, Hybrid MA-TCR, or NGM (non-gene modified) T cells for each well were seeded on the plate and cultured in GT-T551 (Takara Bio) supplemented with 300 IU/mL human recombinant IL-2 (Novartis) and 0.6% autologous plasma. Cells were collected every 48 hours, and the cell count was adjusted to 5×10^5 MA-CAR, HybridMA-TCR, or NGM T cells for each well before reseeding onto new pre-coated wells. On day 8, cells were collected for phenotypic staining and functional assays.

Measurement of the oxygen consumption rate

The oxygen consumption rate (OCR) was measured using a Seahorse XF Cell Mito Stress Test Kit (Agilent Technologies) and a Seahorse XF HS Mini Analyzer.[30] Briefly, 2.5×10^5/well MA-CAR or Hybrid MA-TCR T cells, before chronic stimulation and after chronic antigen stimulation, were seeded into cell culture plates with assay medium and cultured in a 37°C, CO_2-free incubator for 50–60 min until analysis. The final concentrations of oligomycin, FCCP, and rotenone/antimycin A are 1.5, 1.0, and 0.5 µM, respectively.

In vivo antitumor activity

NOD/Shi-scid/IL-2Rγnull (NOG) mice were subcutaneously injected with NW-MEL-38 tumor cells (2.5×10^6 or 3×10^6 or 5×10^6 cells) on day 0, followed by intravenous injections of MA-CAR-T cells, Hybrid MA-TCR-T cells, NGMC, and PBS (−) on days 4, 14, and 29. Tumor growth was measured using calipers and calculated as tumor volume=(length×width^2)/2. When the tumors reached a maximum diameter of 20 mm, the mice were humanely euthanized according to our institutional policy.

Ex vivo assay

NOG mice were inoculated subcutaneously with NW-MEL-38 (5×10^6 cells) on day 0, followed by an intravenous injection of MA-CAR-T cells or Hybrid MA-TCR-T cells on day 29. Tumors (day 37) or spleens (day 43) were collected and lysed from NOG mice transferred with MA-CAR or Hybrid MA-TCR T cells. The tumor tissue was minced and mixed with 10 mL HBSS containing 10 mg/mL of collagenase (Bio-Rad) and incubated at 37°C for 30 min with frequent mixing. The mixture was then filtered through a pre-wet 40 µm strainer. The ACK lysing buffer was used for lysis of red blood cells in murine splenic cells.

Statistical analysis

Data are presented as mean±SD, where error bars are shown. Statistical analyses were performed using unpaired two-tailed Student's t-tests in GraphPad Prism V.10. The significance level was set at $p<0.05$.

RESULTS

Structure of Hybrid MA-TCR and successful transduction into human T cells

We previously reported that MAGE-A4 pMHC-targeted CAR-T (MA-CAR-T) cells using the GITR intracellular domain (ICD) have superior in vitro and in vivo functions compared with those using CD28 or 4-1BB ICD.[11] In this study, we focused on MA-CAR-T cells with GITR ICD for a comparative analysis with Hybrid MA-TCR-T cells (figure 1A). To create Hybrid MA-TCR-T cells with the same scFv antibody as MA-CAR-T cells, we constructed a retroviral vector expressing Hybrid MA-TCR, combining human TCR Cα and Cβ with the identical human scFv antibody VL and VH (Hybrid MA-TCR (LH)) (figure 1B).

We then determined whether Hybrid MA-TCR (LH) could be transduced into human T cells. As shown in figure 1C, the tetramer staining assay confirmed the successful transduction of Hybrid MA-TCR (LH) into human CD8$^+$ and CD4$^+$ T cells. Although the number of Hybrid MA-TCR molecules was significantly lower than that of MA-CAR (figure 1C,D), Hybrid MA-TCR-T cells could recognize T2 cells loaded with a lower amount of MAGE-A4$_{p230-239}$ peptide compared with MA-CAR-T cells (EC_{50} 0.373 nM vs 1.885 nM), indicating improved antigen sensitivity of Hybrid MA-TCR-T cells (figure 1E). Notably, we observed no auto-activation of Hybrid MA-TCR-T cells under non-stimulation conditions, while comparable

activation of Hybrid MA-TCR-T cells and MA-CAR-T cells was observed under stimulation conditions, as measured by CD69 expression (figure 1F).

We also attempted to construct another retroviral vector expressing CAR in which the antibody VH and VL domains were combined with TCR Cα and Cβ, respectively (Hybrid MA-TCR (HL)) (online supplemental figure S1A). However, these CAR-T cells did not recognize MAGE-A4$^+$ HLA-A*02:01$^+$ tumor cell lines (online supplemental figure S1B,C). Consequently, we used Hybrid MA-TCR (LH) for subsequent functional assays.

Hybrid MA-TCR-T cells show superior functional capacities to MA-CAR-T cells in vitro

Next, we investigated the functional capacities of Hybrid MA-TCR-T cells compared with MA-CAR-T cells in vitro. For the cytotoxicity assay, we used SK-MEL-37 (MAGE-A4$^+$ HLA-A*02:01$^+$) and HCT116 (MAGE-A4$^-$ HLA-A*02:01$^+$) melanoma cell lines as targets. As shown in figure 2A, mock-transduced T-cells without genetic modifications (NGMC) did not exhibit any reactivity against these tumor cell lines. In contrast, both Hybrid MA-TCR-T cells and MA-CAR-T cells lysed SK-MEL-37 cells, but not HCT116 cells. Comparable cytotoxic activities were observed using a real-time cytolytic analyzer over a longer period (figure 2B).

Both types of CAR-T cells were further compared regarding cytokine secretion on interaction with MAGE-A4$^+$ HLA-A*02:01$^+$ tumor cells. As shown in figure 2C, both types of CAR-T cells secreted IFN-γ when cocultured with SK-MEL-37, but not HCT116. Notably, Hybrid MA-TCR-T cells secreted significantly more IFN-γ, granzyme B, and TNF-α compared with MA-CAR-T cells (figure 2C online supplemental figure S2). Moreover, ICS analysis revealed a higher proportion of Hybrid MA-TCR-T cells secreting IFN-γ compared with MA-CAR-T cells (figure 2D).

In summary, Hybrid MA-TCR-T cells efficiently recognized the endogenously derived MAGE-A4 peptide in the context of HLA-A*02:01, showing comparable cytotoxic activity, but significantly higher cytokine production than MA-CAR-T cells.

Hybrid MA-TCR-T cells retain strict antigen specificity

Given the potential risk of altered antigen specificity due to genetic recombination and the increased antigen sensitivity of Hybrid MA-TCR-T cells, we evaluated their antigen specificity. We first conducted an IFN-γ ELISPOT assay to determine the reactivity of Hybrid MA-TCR-T cells to T2 cells pulsed with a series of MAGE-A4$_{p230-239}$ analogous peptides, each substituted with alanine at different positions (figure 3A). As shown in figure 3B, the alanine substitution assay revealed that amino acid residues at positions 1–6 and 8 of the MAGE-A4$_{p230-239}$ peptide (GVYDGREHTV) were critical for recognition by Hybrid MA-TCR-T cells. To perform a more detailed analysis, we further conducted an IFN-γ ELISPOT assay to investigate the reactivity of Hybrid MA-TCR-T cells against T2 cells
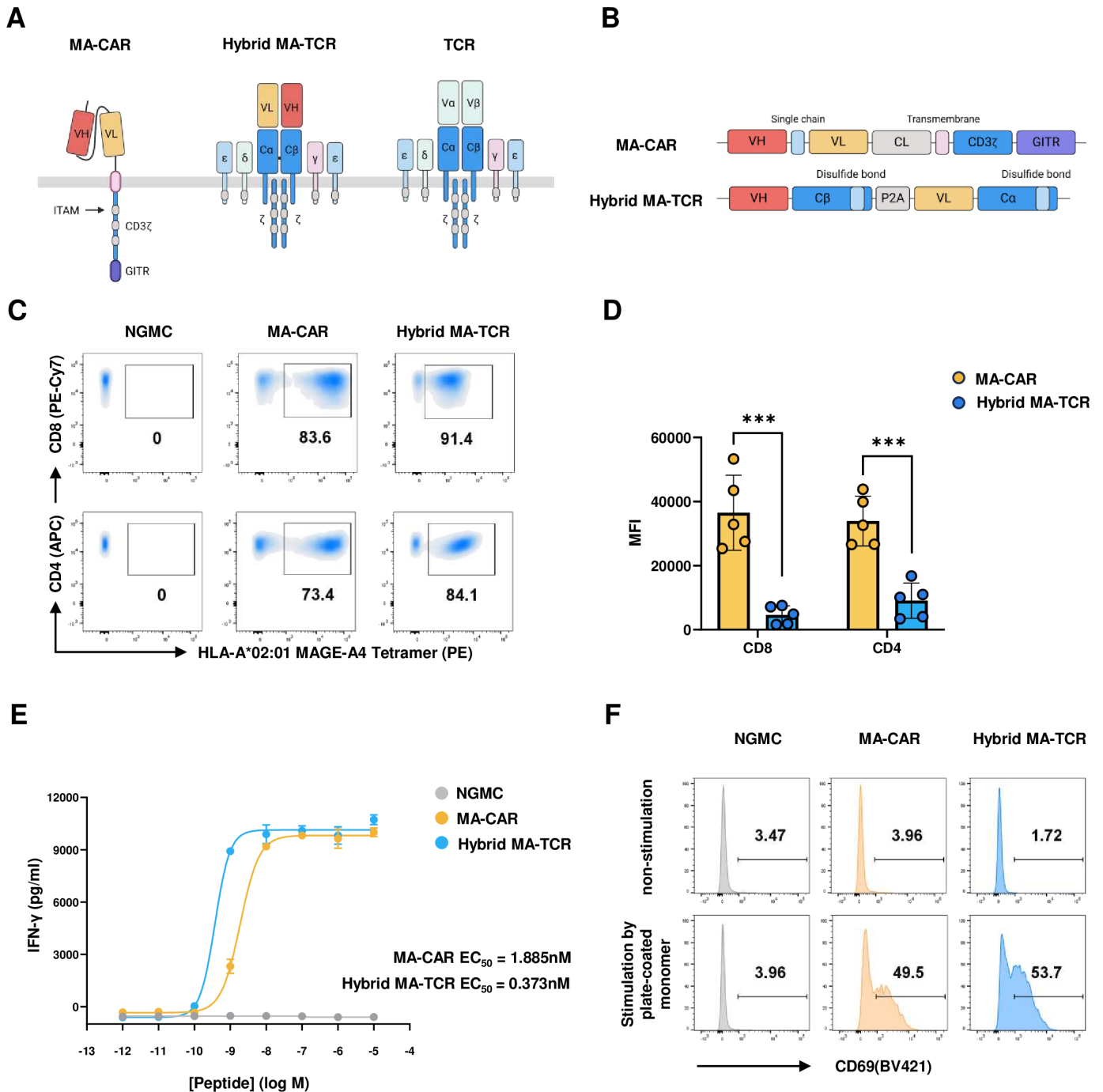
Figure 1 Structure of Hybrid MA-TCR and successful transduction into human T cells. (A) Structure of the predicted Hybrid MA-TCR and its differences from MA-CAR or TCR. (B) Constructs of MA-CAR and Hybrid MA-TCR. (C) Surface expression of MA-CAR or Hybrid MA-TCR in CD8$^+$ and CD4$^+$ T cells. Transfection of MA-CAR or Hybrid MA-TCR vectors into peripheral blood mononuclear cells derived from healthy donors and expansion in the presence of IL-2. Transduction efficiency was determined by the percentage of MA-CAR or Hybrid MA-TCR on the cell surface using MAGE-A4$^+$/HLA-A*02:01 PE-Tetramers staining. (D) Surface expression level of MA-CAR or Hybrid MA-TCR measured by mean fluorescence intensity (MFI). Data represent more than three independent experiments in three independent donors, plotted as mean±SD. (E) NGMC, MA-CAR, or Hybrid MA-TCR T cells were cocultured with T2 target cells pulsed with the MAGE-A4$_{p230-239}$ (GVYDGREHTV) peptide at different peptide concentrations at an effector-to-target ratio of 1:1 for 24 hours. The half maximal effective concentration (EC$_{50}$) value was determined by measuring IFN-γ in the supernatant using an ELISA assay (n=2 per group). (F) Activation of NGMC, MA-CAR, or Hybrid MA-TCR T cells was assessed by measuring CD69 expression after antigen stimulation. NGMC, MA-CAR, and Hybrid MA-TCR T cells on day 10 were stimulated with plate-coated MAGE-A4 monomer (1 µg/mL) or PBS (–) for 48 hours. The activation level was determined by measuring the activation marker CD69 expression using flow cytometry. P values were determined by unpaired t-test (two-tailed). *p≤0.05; **p≤0.01; ***p≤0.001; ****p≤0.0001; not significant (ns) p>0.05. Cα and Cβ, TCR constant α and β; GITR, glucocorticoid-induced TNFR-related protein; IL, interleukin; ITAM, immunoreceptor tyrosine-based activation motif; TCR, T-cell receptor; VH, heavy chain; VL, light chain; Vα and Vβ, TCR variable α and β.
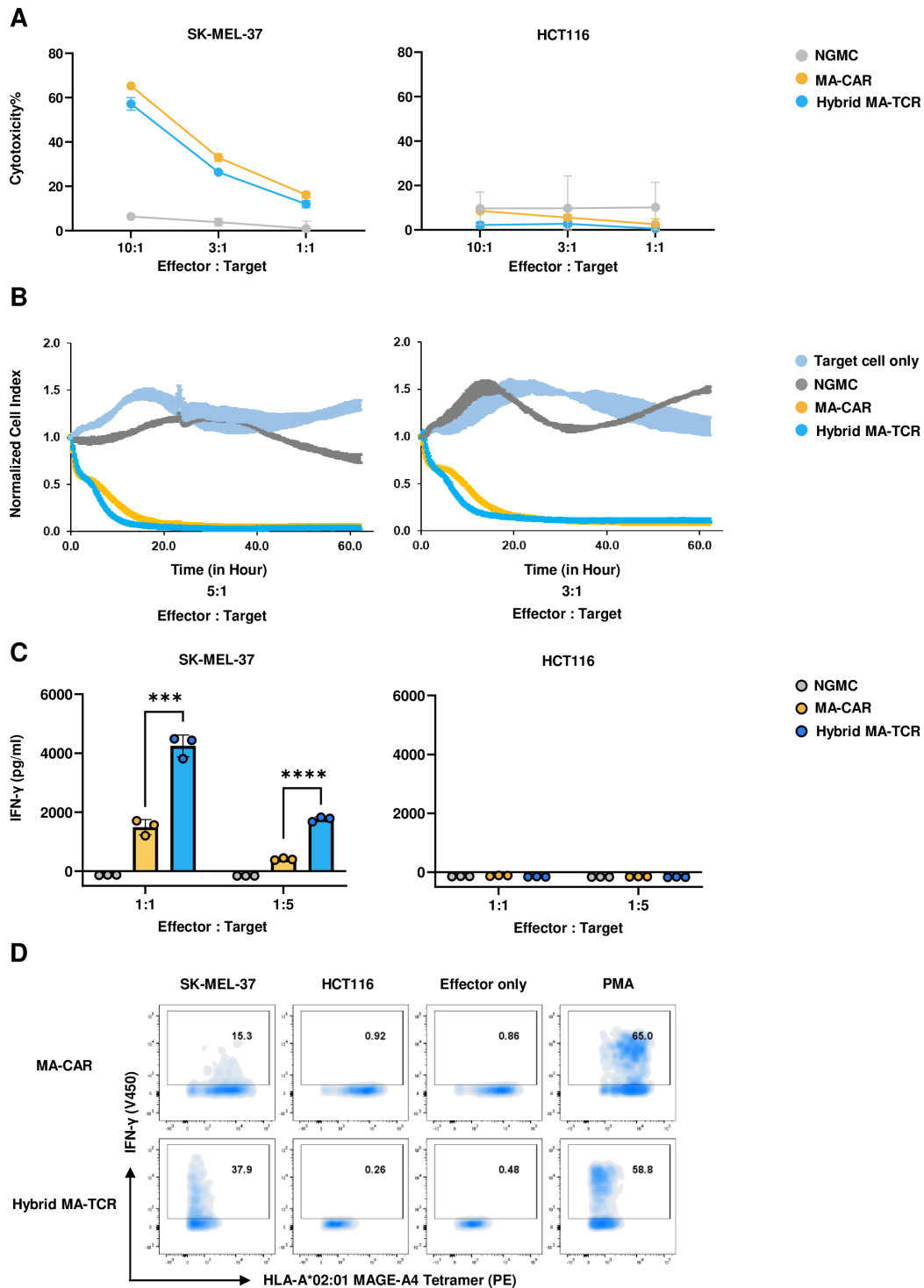
Figure 2 Hybrid MA-TCR-T cells show superior in vitro functions to MA-CAR-T cells. (A) Cellular cytotoxicity assay of NGMC, MA-CAR, and Hybrid MA-TCR T cells coculture with SK-MEL-37 or HCT116 cells at 10:1, 3:1, and 1:1 ratios (effector cells:target cells) for 2 hours using a non-radioactive cellular cytotoxicity assay kit. Data shown as means±SD are technical duplicates from one of three independent experiments. (B) Analysis of NGMC, MA-CAR, and Hybrid MA-TCR T cells' killing function in a long-term cytotoxicity assay based on impedance detection. NGMC, MA-CAR, and Hybrid MA-TCR T cells were cocultured with SK-MEL-37 cells at 5:1 and 3:1 ratios (effector cells:target cells). SK-MEL-37 lysis was measured in an impedance-based real-time cytotoxicity assay. Data are representative of two independent experiments and shown as means±SD. (C) Detection of IFN-γ secretion by NGMC, MA-CAR, and Hybrid MA-TCR T cells following a 24 hours coculture with SK-MEL-37 or HCT116 cells at 1:1 and 1:5 ratios (effector cells:target cells). Measurement of supernatant IFN-γ levels by ELISA. Data are means±SD of three experimental replicates. (D) Intracellular staining of IFN-γ in MA-CAR and Hybrid MA-TCR T cells after a 5 hours coculture with SK-MEL-37 cells, HCT116 cells, RPMI medium only, or PMA and Ionomycin for 5 hours. Frequency of IFN-γ+ cells in MA-CAR+ or Hybrid MA-TCR+ populations are indicated within the dot plot. IFN-γ, interferon-gamma; PMA, phorbol 12-myristate 13-acetate.

A

Alanine substitution analysis

MAGE-A4	G V Y D G R E H T V
1A	A V Y D G R E H T V
2A	G A Y D G R E H T V
3A	G V A D G R E H T V
4A	G V Y A G R E H T V
5A	G V Y D A R E H T V
6A	G V Y D G A E H T V
7A	G V Y D G R A H T V
8A	G V Y D G R E A T V
9A	G V Y D G R E H A V
10A	G V Y D G R E H T A

B

C

	G	V	Y	D	G	R	E	H	T	V
	1	2	3	4	5	6	7	8	9	10
A	0.044335	0.014778	0.009852	0.014778	0.004926	0.044335	0.320197	0.024631	0.921182	0.793103
C	0.026786	0	0	0.5625	0.008929	0.017857	0.860104	0.003454	1.1019	0.059375
D	0.071429	0.008929	0.017857	1	0.035714	0.035714	0.001727	0.001727	0.911917	0
E	0.008929	0.008929	0.017857	0.008929	0.026786	0.008929	1	0.005181	1.027634	0.08981
F	0	0.008929	0	0.008929	0.026786	0.003454	0.001727	0.034542	0.932642	0.614853
G	1	0.026786	0.008929	0	1	0.008636	0.006908	0.006908	0.889465	0.005181
H	0.044643	0.008929	0.008929	0.017857	0.008929	0.001727	0.055268	1	1.112263	0
I	0.017857	1.446429	0	0.008929	0.026786	0.006908	0.008636	0.005181	1.036269	0.006908
K	0.026786	0.008929	0.026786	0	0.008929	0.003454	0.01209	0.003454	1.034542	0.003454
L	0.008929	0.008929	0.035714	0.017857	0.026786	0.001727	0.053541	0.003454	0.943005	0
M	0.017857	0.008929	0.008929	0.008929	0	0.008636	1.172712	1.072539	0.994819	0.901554
N	0.026786	0.017857	0.017857	0.008929	0.017857	0.003454	0.003454	0.003454	0.97582	0.008636
P	0.017857	0.008929	0.017857	0.017857	0.026786	0.006908	0.039724	0.001727	0.873921	0.003454
Q	0	0.026786	0.035714	0.026786	0.008929	0.001727	1.146805	0.084629	0.901554	0
R	0	0.008929	0.017857	0	0.026786	1	0.217617	1.008636	1.036269	0.001727
S	0	0	0.008929	0.035714	0	0.006908	0.297064	0.005181	1.072539	0.043178
T	0	0.008929	0	0.035714	0.035714	0.006908	0.01209	0.001727	1	1.183074
V	0.035714	1	0.008929	0.035714	0.008929	0.006908	0	0.003454	1.062176	1
W	0.026786	0.008929	0.526786	0.026786	0	0.008636	0.015544	1.058722	0.784111	0.008636
Y	0	0.026786	1	0.026786	0.455357	0.003454	1.027634	0.521589	0.986183	0

Permissive amino acids

G	V	Y	D	G	R	X	X	X	X
	I	W	C	Y					

Figure 3 Hybrid MA-TCR-T cells maintain strict antigen specificity. (A) Schematic representation of the alanine substitution analysis. (B) Hybrid MA-TCR T cells were analyzed for their recognition of MAGE-A4$_{p230-239}$ peptide residues using alanine substitution analysis. The MAGE-A4$_{p230-239}$ peptide sequence was substituted with alanine at residues 1 through 10. T2 peptide-pulsed cells and effector cells were seeded into anti-human IFN-γ monoclonal antibody (1-D1K; Mabtech) pre-coated plates at an E:T ratio of 1:1 and assayed for IFN-γ by enzyme-linked immunosorbent spot (ELISpot). Data are representative of three independent experiments and shown as means. (C) Potential cross-reactivity of Hybrid MA-TCR T cells was identified through comprehensive amino acid substitution analysis. The MAGE-A4$_{p230-239}$ peptide was substituted with all 20 amino acids. Hybrid MA-TCR T cells were cultured with T2 cells pulsed with these peptides and assayed through an IFN-γ ELISPOT assay. The percentage data shown in the heatmap in the upper panel were calculated as follows: (experimental spot counts)/(parental MAGE-A4$_{p230-239}$ spot counts). Permissible amino acid residues were defined (lower panel) based on a 0.1 (10%) cut-off value. Data are representative of two independent experiments and shown as means. IFN-γ, interferon-gamma.

pulsed with an array of MAGE-A4$_{p230-239}$ analogous peptides, each substituted at every position with all 20 amino acids. The results showed that a few amino acid substitutions in the N-terminal contiguous 6-amino acid sequence were permissive for MAGE-A4 pMHC recognition by the Hybrid MA-TCR-T cells (figure 3C). These findings are consistent with those previously reported by our group for MA-CAR-T

cells.[11] Thus, we concluded that Hybrid MA-TCR-T cells retain strict antigen specificity, despite genetic modifications.

In vitro functional superiority of Hybrid MA-TCR-T cells to MA-CAR-T cells becomes more pronounced on repetitive antigen stimulation

Chronic CAR activation via engagement with the target antigen causes CAR-T dysfunction, resulting in clinical in vivo failure.[31–33] Hence, we performed an in vitro comparative functional analysis of Hybrid MA-TCR-T cells and MA-CAR-T cells using a protocol of repetitive antigen stimulation that mimicked in vivo conditions (figure 4A).[34] Plate-bound MAGE-pMHC monomers were used to stimulate both types of CAR-T cells. Two days after the fourth stimulation, these CAR-T cells were analyzed for PD-1, TIM3, and LAG3 expression. As shown in figure 4B, fully exhausted CAR-T cells (PD-1$^+$TIM3$^+$LAG3$^+$) were more abundant in MA-CAR-T cells than in Hybrid MA-TCR-T cells, indicating the relative resistance to exhaustion of Hybrid MA-TCR-T cells.

Next, we assessed cytotoxic activity and IFN-γ production after repetitive antigen stimulation. Despite comparable cytotoxic function under conventional conditions (figure 2A,B), we found that Hybrid MA-TCR-T cells exhibited significantly higher cytotoxic activity and IFN-γ production than MA-CAR-T cells (figure 4C,D).

We then conducted a phenotypic analysis of these CAR-T cells with respect to memory formation because the memory phenotypes of infused CAR-T cells have been reported to predict CAR-T cell persistence in vivo.[35–37] Both types of CAR-T cells exhibited a naïve-like phenotype (CD62L$^+$CD45RA$^+$) in both CD8$^+$ and CD4$^+$ cells before stimulation. However, most MA-CAR-T cells exhibited an effector phenotype (CD62L$^-$CD45RA$^+$) after repetitive antigen stimulation. In contrast, the Hybrid MA-TCR-T cells were still rich in naïve (CD62L$^+$CD45RA$^+$) and central memory T cells (CD62L$^+$CD45RA$^-$) (figure 4E). These results suggest that MA-CAR-T cells differentiate into effector cells on repeated antigen stimulation, many of which become exhausted.

Consistent with these results, Hybrid MA-TCR-T cells showed a higher spare-respiratory capacity than MA-CAR-T cells after repetitive antigen stimulation, whereas both types of CAR-T cells showed comparable OCRs before stimulation (figure 4F).

Overall, Hybrid MA-TCR-T cells exhibited superior in vitro functional capacities compared with MA-CAR-T cells with respect to cytotoxicity, cytokine production, reduced exhaustion, memory phenotype, and mitochondrial function after repetitive stimulation with antigens.

Hybrid MA-TCR-T cells exhibit higher therapeutic efficacy than MA-CAR-T cells

The observed superior in vitro functionalities of Hybrid MA-TCR-T cells encouraged us to evaluate their therapeutic efficacy using a xenograft model with immunodeficient NOD/Shi-scid/IL-2Rγnull (NOG) mice. We

adoptively transferred 2.5×10^6 effector T cells (Hybrid MA-TCR-T, MA-CAR-T, NGMC), prepared from an identical healthy donor, 4 days after subcutaneous inoculation with 2.5×10^6 NW-MEL-38 (MAGE-A4$^+$ HLA-A*02:01$^+$) tumor cells (figure 5A). As expected, the adoptive transfer of Hybrid MA-TCR-T cells or MA-CAR-T cells significantly suppressed the growth of NW-MEL-38 cells. Surprisingly, Hybrid MA-TCR-T cells eradicated tumors in all four mice tested, demonstrating significantly higher therapeutic efficacy than MA-CAR-T cells (figure 5B,C).

We then examined the minimum number of Hybrid MA-TCR-T cells required for tumor eradication under more stringent experimental conditions. For this purpose, we adoptively transferred different numbers of Hybrid MA-TCR-T cells (3×10^6, 1×10^6, and 3×10^5) into NOG mice 14 days after subcutaneous inoculation with 5×10^6 NW-MEL-38 tumor cells (figure 5D). We observed that even 3×10^5 Hybrid MA-TCR-T cells significantly inhibited tumor growth, and 1×10^6 Hybrid MA-TCR-T cells eradicated established tumors in all mice tested (figure 5E,F). Collectively, the Hybrid MA-TCR-T cells showed significantly higher therapeutic efficacy than the MA-CAR-T cells. Notably, in these experiments, no symptoms suggestive of GVHD, such as decreased body weight, were observed (online supplemental figure S3).

High infiltration of functional Hybrid MA-TCR$^+$-T cells in tumor tissue might dictate their superior therapeutic efficacy

The unexpectedly high therapeutic efficacy of Hybrid MA-TCR-T cells prompted us to investigate the in vivo differences between the two types of CAR-T cells, especially in tumor tissues. 12 NOG mice were transplanted with 5×10^6 NW-MEL-38 tumor cells on day 0. When the mean tumor volume reached approximately 500 mm^3 (on day 29), either 3×10^6 Hybrid MA-TCR-T or MA-CAR-T cells were injected into the mice (each group consisted of six mice) (figure 6A). Both CAR-T cell types were prepared from the same healthy donor and showed similar CD4/CD8 ratios and CAR positivity (online supplemental figure S4A,B).

Based on our experience with this mouse model, the difference in tumor size between the effective and ineffective groups became apparent approximately ten days after infusion. As expected, we observed no significant difference in tumor volume 7 days after infusion (day 36) (figure 6B). We promptly analyzed tumor-infiltrating lymphocytes (TILs) collected from three tumors of the same size in each group. Although there was a relatively higher frequency of CD4$^+$ TILs in the Hybrid MA-TCR-T cell group, we observed no significant difference in the total number of TILs (figure 6C). However, the number of CAR$^+$ CD4$^+$ and CD8$^+$ TILs was significantly higher in the Hybrid MA-TCR-T cell group (figure 6D). Notably, the CAR$^+$ TILs in the Hybrid MA-TCR-T cell group were higher than those in the infusion product for both CD4$^+$ and CD8$^+$ cells (online supplemental figure S4C). These results might indicate higher trafficking of CAR$^+$T cells into tumor tissues in this group. Unexpectedly, we
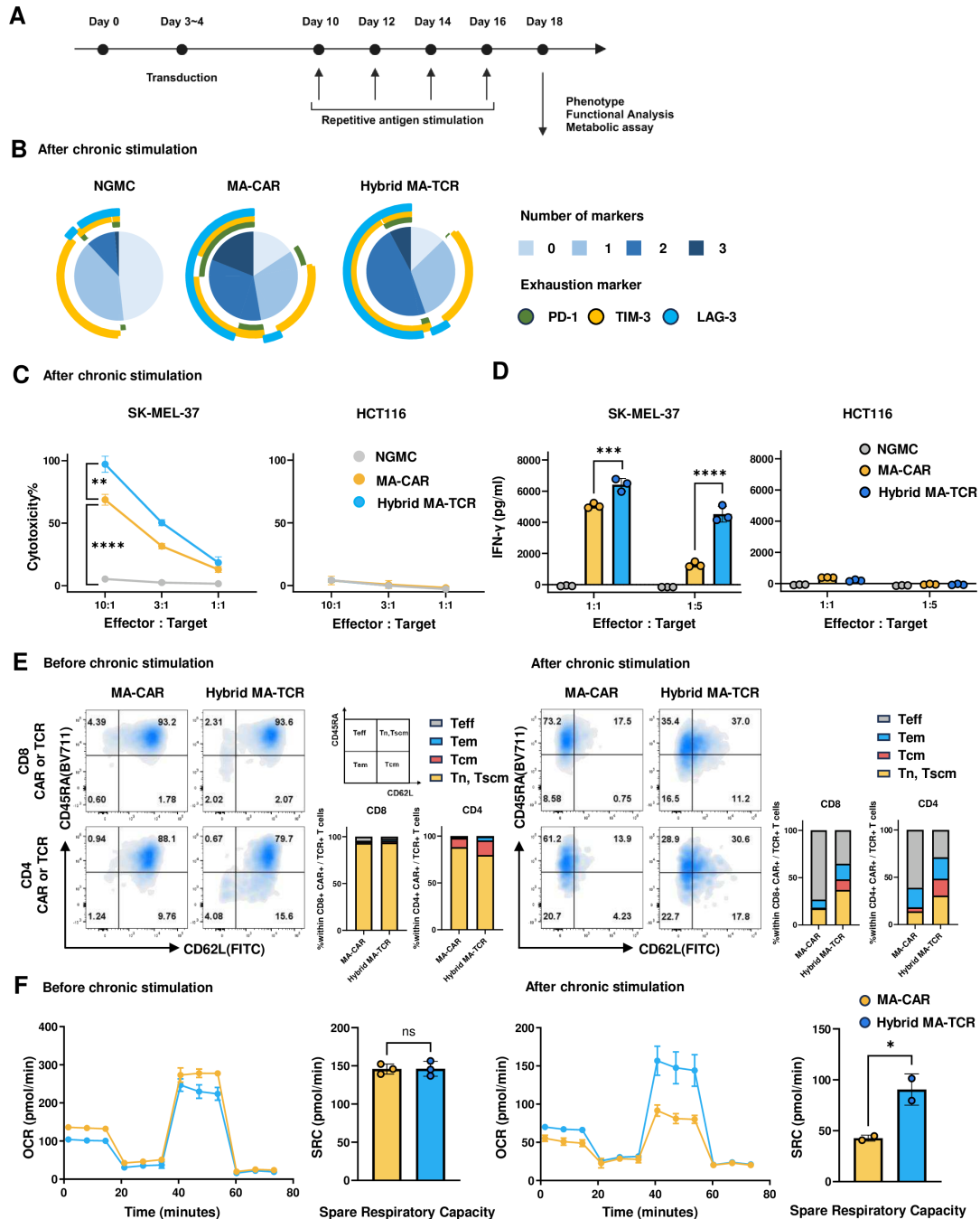
Figure 4 Functional superiority of Hybrid MA-TCR-T cells becomes more pronounced on chronic antigen stimulation. (A) Experimental schematic for four rounds of antigen stimulation. NGMC, MA-CAR, or Hybrid MA-TCR T cells were stimulated by plate-coated MAGE-A4 monomer (1 µg/mL). Cells were collected every 48 hours, standardized by cell number, and placed onto a new MAGE-A4 monomer-coated plate. (B) Representative data of PD-1, TIM-3, and LAG-3 expression in NGMC, MA-CAR, or Hybrid MA-TCR T cells through flow cytometry after 8 days of four rounds of antigen stimulation. (C) After four rounds of antigen stimulation, a cellular cytotoxicity assay was performed with NGMC, MA-CAR, and Hybrid MA-TCR T cells cocultured with SK-MEL-37 or HCT116 cells at 10:1, 3:1, and 1:1 ratios (effector cells:target cells) for 2 hours using a non-radioactive cellular cytotoxicity assay kit. (D) After four rounds of antigen stimulation, IFN-γ secretion by NGMC, MA-CAR, and Hybrid MA-TCR T cells was detected following 24 hours coculture with SK-MEL-37 or HCT116 cells at 1:1 and 1:5 ratios (effector cells:target cells). Measurement of supernatant IFN-γ levels by ELISA. (C, D) Data shown as means±SD are technical duplicates from one of three independent experiments. (E) Before or after four rounds of antigen stimulation, representative data of the memory phenotype CD45RA and CD62L expression in MA-CAR⁺ or Hybrid MA-TCR⁺ T cells through flow cytometry. The left panel shows the representative FACS data, and the right panel shows the statistical summary. (F) Before or after four rounds of antigen stimulation, mitochondrial stress and changes in oxygen consumption rate and the spare respiratory capacity level were analyzed using a Seahorse XF Cell Mito Stress Test Kit. Data are representative of two independent experiments and shown as means±SD. P values were determined by unpaired t-test (two-tailed). *p≤0.05; **p≤0.01; ***p≤0.001; ****p≤0.0001; not significant (ns) p>0.05. IFN-γ, interferon-gamma.
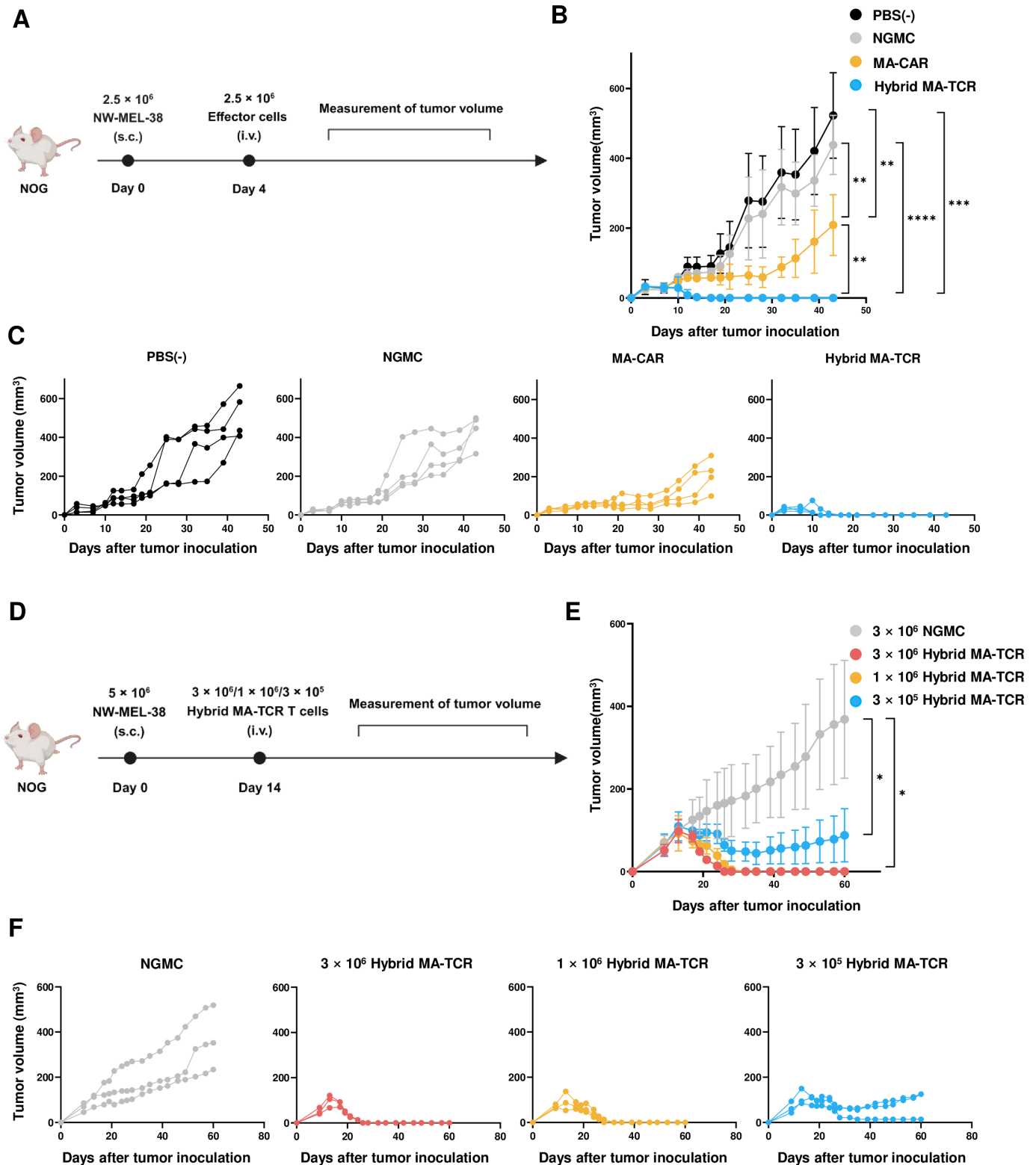
Figure 5 Hybrid MA-TCR-T cells exhibit higher therapeutic efficacy than MA-CAR-T cells. (A, D) Schematic representation of the adoptive transfer experiment using NOG mice. (B, C) Tumor growth curves for the NOG mouse model. In this model, 2.5×10^6 NW-MEL-38 (MAGE-A4+/HLA-A*02:01+) cells were inoculated subcutaneously (s.c.) on the back of each mouse. NGMC 2.5×10^6 (gray), MA-CAR (yellow), Hybrid MA-TCR (blue) T cells, or PBS (–) (black) were injected intravenously on day 4 after tumor inoculation (n=4 per group). (C) Tumor growth curves for each mouse. (E, F) Tumor growth curves for the NOG mouse model. In this model, 5×10^6 NW-MEL-38 cells were inoculated s.c. on the back of each mouse. NGMC (3×10^6) (gray), 3×10^6 Hybrid MA-TCR (red), 1×10^6 Hybrid MA-TCR (yellow), or 3×10^5 Hybrid MA-TCR (blue) T cells were injected intravenously on day 14 after tumor inoculation (n=3 per group). (F) Tumor growth curves for each mouse. (B, E) Data are shown as means±SD. P values were determined by unpaired t-test (two-tailed). *p≤0.05; **p≤0.01; ***p≤0.001; ****p≤0.0001; not significant (ns) p>0.05.
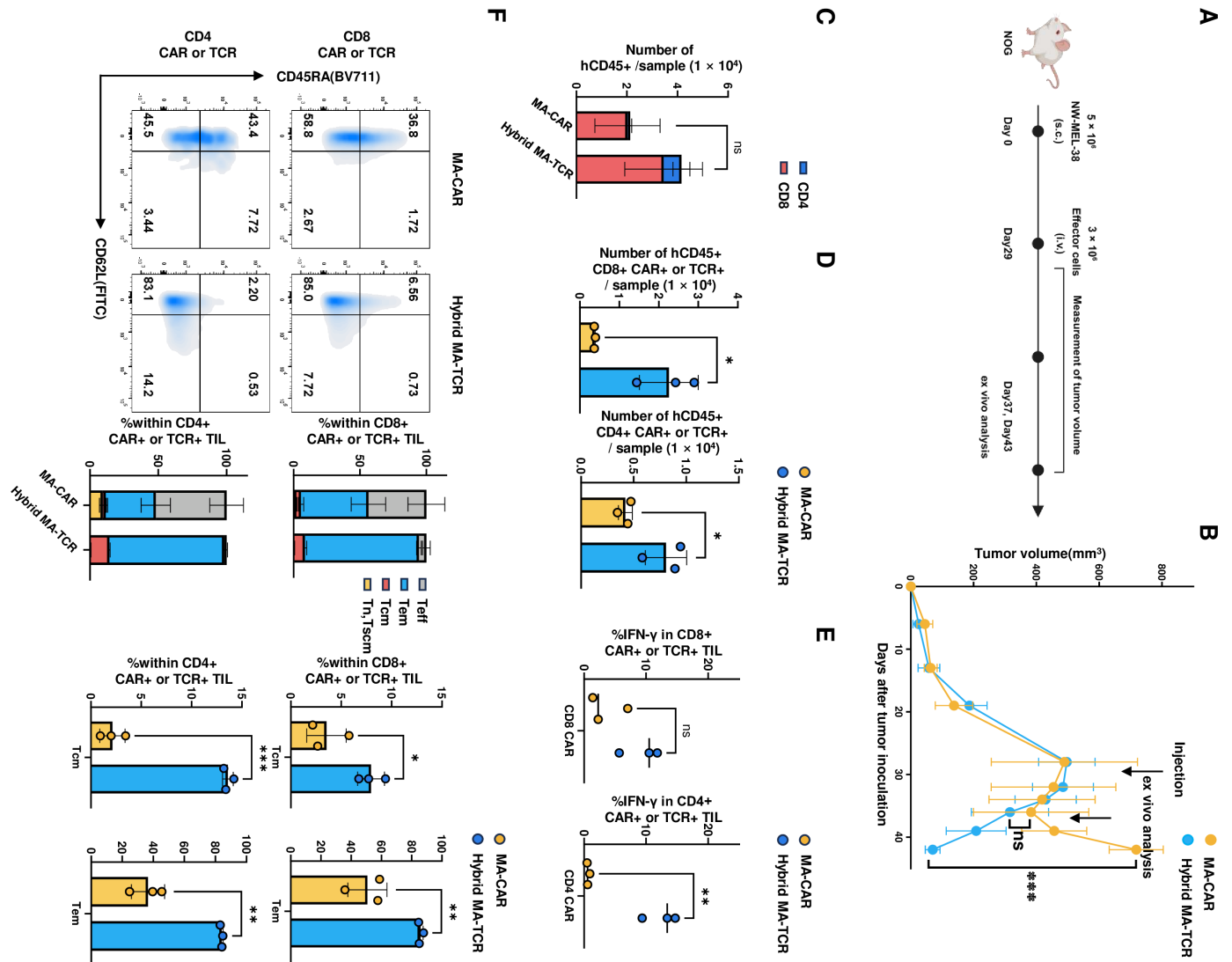
Figure 6 Higher infiltration of functional Hybrid MA-TCR-T cells in tumor tissues. (A) Schematic of the ex vivo CAR or Hybrid TCR-T cell analysis. In the NOG mouse model, 5×10^6 NW-MEL-38 cells were inoculated s.c. on the back of each mouse. MA-CAR 3×10^6 or Hybrid MA-TCR T cells were injected intravenously on day 29 after tumor inoculation. Tumors (day 37) or spleens (day 43) were collected and lysed from NOG mice transferred with MA-CAR or Hybrid MA-TCR T cells. (B) Growth curves of NW-MEL-38 tumors in the NOG mouse model. (C) Quantification of human-CD45 cells in tumor tissues. On day 37, tumor tissues were collected and lysed from NOG mice transferred with MA-CAR or Hybrid MA-TCR T cells. Comparison of the human-CD45 number for each sample within TILs was done using flow cytometry. (n=3 per group, each dot=one mouse) (D) Quantification of human-CD45$^+$ CD8$^+$ CAR$^+$/TCR$^+$ or human-CD45$^+$ CD4$^+$ CAR$^+$/TCR$^+$ cells in tumor tissues. On day 37, the human-CD45$^+$ CD8$^+$ CAR$^+$/TCR$^+$ or human-CD45$^+$ CD4$^+$ CAR$^+$/TCR$^+$ cell numbers for each sample within TILs were compared using flow cytometry (n=3 per group, each dot=one mouse). (E) Quantification of IFN-γ in the human-CD45$^+$ CD8$^+$ CAR$^+$/TCR$^+$ or human-CD45$^+$ CD4$^+$ CAR$^+$/TCR$^+$ cells in tumor tissues. On day 37, lysed tumor tissue cells were treated with GolgiStop Protein Transport Inhibitor and incubated for an additional 4 hours, followed by permeabilization/fixation and subsequent IFN-γ staining. IFN-γ detection in the human-CD45$^+$ CD8$^+$ CAR$^+$/TCR$^+$ or human-CD45$^+$ CD4$^+$ CAR$^+$/TCR$^+$ populations was performed using flow cytometry (n=3 per group, each dot=one mouse). (F) On day 37, the memory phenotype (CD45RA and CD62L expression) of MA-CAR$^+$ or Hybrid MA-TCR$^+$ T cells from tumor tissues was analyzed using flow cytometry (n=3 per group, each dot=one mouse). The left panel shows representative FACS data, and the right panel shows the statistical summary. (B–F) Data are shown as means±SD, each dot=one mouse. P values were determined by unpaired t-test (two-tailed). *p≤0.05; **p≤0.01; ***p≤0.001; ****p≤0.0001; not significant (ns) p>0.05. IFN-γ, interferon-gamma; s.c., subcutaneously; TILs, tumor-infiltrating lymphocytes.

observed that CD4$^+$ MA-CAR$^+$-TILs barely secreted IFN-γ, although no significant difference in IFN-γ production was observed in CD8$^+$ CAR$^+$-TILs from the two groups (figure 6E). This result indicates that CD4$^+$ MA-CAR$^+$TILs became dysfunctional in vivo at this time point.

Phenotypic analysis revealed that the frequency of central memory (CD62L$^+$CD45RA$^-$) and effector memory (CD62L$^-$CD45RA$^-$) populations were significantly higher in Hybrid MA-TCR$^+$-TILs than in MA-CAR$^+$-T TILs (figure 6F). Based on these results, we examined splenic

cells from both groups on day 43 to evaluate the longevity of CAR$^+$T cells. As expected, the number of splenic CD4$^+$ and CD8$^+$ Hybrid MA-TCR$^+$ T cells was significantly higher than that of the MA-CAR-T group. These results might indicate a longer persistence of Hybrid MA-TCR$^+$-T cells (online supplemental figure S4D,E).

Collectively, these results suggest that higher infiltration of Hybrid MA-TCR$^+$-T cells exhibiting functional and memory phenotypes in tumor tissues might be one mechanism underlying their superior therapeutic efficacy.

DISCUSSION

With technological advancements, various innovations in CAR constructs have been made to improve the in vivo efficacy of CAR-T cells.[38] Among these, CAR constructs incorporating the TCR machinery have recently attracted attention, although the fundamental concept was originally proposed by Kuwana *et al* and Gross *et al* in the late 1980s.[39 40]

In this study, we aimed to determine whether MAGE-A4 pMHC-targeted CAR-T cells exploiting the TCR machinery (Hybrid MA-TCR-T cells) exhibit superior functionality compared with MAGE-A4 pMHC-targeted CAR-T cells (MA-CAR-T cells). Indeed, the results demonstrated that Hybrid MA-TCR-T cells exhibited superior functions compared with those of MA-CAR-T cells, without altering their strict antigen specificity. Particularly, a series of in vivo experiments demonstrated significantly higher efficacy of Hybrid MA-TCR-T cells than MA-CAR-T cells. These results prompted us to investigate the reasons for the significant in vivo function of Hybrid MA-TCR-T cells.

TIL analyses revealed that the high infiltration of functional Hybrid MA-TCR$^+$-T cells exhibiting a less-differentiated phenotype into the tumor tissue might dictate this superior in vivo function. Conversely, we observed unexpected data showing that CD4$^+$ MA-CAR$^+$-TILs barely secreted IFN-γ, suggesting hyporesponsiveness, dysfunction, or Th2 polarization of these CD4$^+$ MA-CAR$^+$-TILs. This result is noteworthy because tumor-specific CD4$^+$ TILs are known to play multifaceted roles, such as enhancing the survival of CD8$^+$ T cells and recruiting CD8$^+$ T cells to tumor sites through IFN-γ-dependent production of chemokines.[41 42] In our previous study, CD4$^+$ MA-CAR$^+$T cells attenuated the in vivo efficacy of CD8$^+$ MA-CAR$^+$T cells via undefined mechanisms.[11] Although the experimental design and assay time points of the previous and current studies were different, these dysfunctional CD4$^+$ MA-CAR-TILs could contribute to the understanding of lower in vivo efficacy of MA-CAR-T cells and higher in vivo efficacy of Hybrid MA-TCR$^+$-T cells.

Although unexpected from the in vitro results, one possible explanation for the functional decline observed in CD4$^+$ MA-CAR$^+$TILs is that MA-CAR-T cells might recognize MAGE-A4 pMHC in vivo in a CD8-dependent manner. As shown in this study and previous studies on STAR and HIT,[24 25] we observed a slightly higher antigen sensitivity of Hybrid MA-TCR-T cells than that

of MA-CAR-T cells (EC$_{50}$ 0.373 nM vs 1.885 nM). Hybrid MA-TCR-T cells may recognize MAGE-A4 pMHC in a CD8-independent manner due to the slight increase in antigen sensitivity.

Another possible factor contributing to the striking difference in in vivo efficacy between the two types of CAR-T cells is simply attributed to their CAR density. Previous studies reported that CAR-T cells with high expression of CAR molecules showed increased tonic signaling, resulting in CAR-T cell exhaustion, dysfunction, and lower in vivo efficacy.[43 44] Given that the number of CAR molecules on MA-CAR-T cells was significantly higher than that on Hybrid MA-TCR-T cells (figure 1C,D), MA-CAR-T cells were more susceptible to exhaustion, thus showing lower in vivo efficacy than Hybrid MA-T-CR-T cells. In addition, CAR structures such as AbTCR, TAC, TRuC, and STAR exhibit inherently lower tonic signaling, presumably by exploiting physiological TCR signaling.[21–24] Although no data showed reduced tonic signaling in this study, this factor may have affected the in vivo outcomes. Regarding T cell signaling, which determines cell fate and efficacy, the previous study has reported that EGFR-targeting STAR-T cells showed gene expression patterns more similar to TCR-T cells after antigen stimulation than CAR-T cells. Given that the TCR machinery is evolutionarily optimized for pMHC recognition and that Hybrid-TCR-T cells recognize pMHC at the same antigen density as TCR-T cells, Hybrid-TCR-T cells targeting pMHC may exhibit a more similar gene expression profile to TCR-T cells after pMHC recognition, resulting in increased in vivo efficacy. Although speculative, pMHC-targeting CARs may have more advantages over conventional CARs when using the TCR machinery. Overall, many factors may influence the in vivo efficacy of Hybrid MA-TCR-T and MA-CAR-T cells. A more detailed analysis is required to address these issues.

A comprehensive analysis revealed similar antigen specificity between the Hybrid MA-TCR-T and MA-CAR-T cells. However, the risk of cross-reactivity between Hybrid MA-TCR-T cells and self-peptides, possibly caused by mispairing between the endogenous TCR and introduced chimeric chains, cannot be ignored. To mitigate this risk, several strategies, such as the usage of γδ constant chain (AbTCR),[21] murine TCR constant chain (STAR),[24] deletion of endogenous TCR (HIT),[25] or suppression of endogenous TCR by siRNA,[45] would be practical choices.

The present results indicate that pMHC-targeted CAR-T cells exploiting the TCR machinery exhibit enhanced in vitro and in vivo functions without altering antigen specificity in the experimental setting of this study. We acknowledge the limitations of this study based on one pMHC-targeted CAR, but the obtained results could be applicable to other pMHC-targeted CARs, such as shared neoantigen-targeted pMHC CARs.[46 47] In this context, this strategy may facilitate the development of gene-modified T cell therapy for solid tumors. In the case of the development of TCR-T

therapy, it is necessary to first obtain TCR specific for a particular pMHC and then improve affinity of the TCR by amino acids substitution in the complementarity determining regions. Given that it is technically relatively easy to obtain antibodies specific to pMHC by screening from an scFv library, it might be feasible to prepare in advance a panel of viral vectors for expression of Hybrid-TCRs that specifically recognize a variety of shared neoantigen-derived peptide/MHC complexes.

In conclusion, we believe that the present results can help broaden and develop effective pMHC-targeted CAR-T therapy for solid tumors.

Patient consent for publication All authors agreed with publication and none of the data have been previously reported or elsewhere.

Ethics approval Written informed consent was obtained from healthy volunteers in accordance with the guidelines of the Declaration of Helsinki. The experimental protocol was approved by the Institutional Review Board of Mie University School of Medicine (approval no. 3264). Female NOD/Shi-scid/IL-2Rγnull mice, known as NOG mice, were purchased from the Central Institute for Experimental Animals (Kawasaki, Japan). All mice were housed under specific pathogen-free conditions and used at 6–10 weeks of age. All animal experiments were conducted according to protocols approved by the Animal Care and Use Committee of the Mie University Life Science Center (approved no. 23-21).

Provenance and peer review Not commissioned; externally peer reviewed.

Data availability statement Data are available upon reasonable request. Data supporting this study are available from the corresponding author upon request.

Supplemental material This content has been supplied by the author(s). It has not been vetted by BMJ Publishing Group Limited (BMJ) and may not have been peer-reviewed. Any opinions or recommendations discussed are solely those of the author(s) and are not endorsed by BMJ. BMJ disclaims all liability and responsibility arising from any reliance placed on the content. Where the content includes any translated material, BMJ does not warrant the accuracy and reliability of the translations (including but not limited to local regulations, clinical guidelines, terminology, drug names and drug dosages), and is not responsible for any error and/or omissions arising from translation and adaptation or otherwise.

ORCID iDs
Meiou Liu http://orcid.org/0009-0001-5706-2478
Yasushi Akahori http://orcid.org/0000-0002-4053-909X
Naoko Imai http://orcid.org/0009-0008-7055-1875
Linan Wang http://orcid.org/0009-0007-1640-9758
Kohei Negishi http://orcid.org/0009-0008-8137-6566
Takuma Kato http://orcid.org/0000-0001-9140-6644
Hiroshi Fujiwara http://orcid.org/0000-0003-3340-6915
Hiroshi Miwa http://orcid.org/0000-0002-4892-3192
Yoshihiro Miyahara http://orcid.org/0000-0002-6458-3167

REFERENCES

1 Neelapu SS, Locke FL, Bartlett NL, *et al*. Axicabtagene Ciloleucel CAR T-Cell Therapy in Refractory Large B-Cell Lymphoma. *N Engl J Med* 2017;377:2531–44.
2 Maude SL, Laetsch TW, Buechner J, *et al*. Tisagenlecleucel in Children and Young Adults with B-Cell Lymphoblastic Leukemia. *N Engl J Med* 2018;378:439–48.
3 Schmidts A, Maus MV. Making CAR T Cells a Solid Option for Solid Tumors. *Front Immunol* 2018;9:2593.
4 Albelda SM. CAR T cell therapy for patients with solid tumours: key lessons to learn and unlearn. *Nat Rev Clin Oncol* 2024;21:47–66.
5 Del Bufalo F, De Angelis B, Caruana I, *et al*. GD2-CART01 for Relapsed or Refractory High-Risk Neuroblastoma. *N Engl J Med* 2023;388:1284–95.
6 Mackensen A, Haanen JBAG, Koenecke C, *et al*. CLDN6-specific CAR-T cells plus amplifying RNA vaccine in relapsed or refractory solid tumors: the phase 1 BNT211-01 trial. *Nat Med* 2023;29:2844–53.
7 Qi C, Gong J, Li J, *et al*. Claudin18.2-specific CAR T cells in gastrointestinal cancers: phase 1 trial interim results. *Nat Med* 2022;28:1189–98.
8 Andersen PS, Stryhn A, Hansen BE, *et al*. A recombinant antibody with the antigen-specific, major histocompatibility complex-restricted specificity of T cells. *Proc Natl Acad Sci U S A* 1996;93:1820–4.
9 Chames P, Willemsen RA, Rojas G, *et al*. TCR-like human antibodies expressed on human CTLs mediate antibody affinity-dependent cytolytic activity. *J Immunol* 2002;169:1110–8.
10 Akahori Y, Wang L, Yoneyama M, *et al*. Antitumor activity of CAR-T cells targeting the intracellular oncoprotein WT1 can be enhanced by vaccination. *Blood* 2018;132:1134–45.
11 Wang L, Matsumoto M, Akahori Y, *et al*. Preclinical evaluation of a novel CAR-T therapy utilizing a scFv antibody highly specific to MAGE-A4$_{p230-239}$/HLA-A∗02:01 complex. *Mol Ther* 2024;32:734–48.
12 Sterner RC, Sterner RM. CAR-T cell therapy: current limitations and potential strategies. *Blood Cancer J* 2021;11:69.
13 Qin Y, Xu G. Enhancing CAR T-cell therapies against solid tumors: Mechanisms and reversion of resistance. *Front Immunol* 2022;13:1053120.
14 Frigault MJ, Lee J, Basil MC, *et al*. Identification of chimeric antigen receptors that mediate constitutive or inducible proliferation of T cells. *Cancer Immunol Res* 2015;3:356–67.
15 Smith EL, Harrington K, Staehr M, *et al*. GPRC5D is a target for the immunotherapy of multiple myeloma with rationally designed CAR T cells. *Sci Transl Med* 2019;11:eaau7746.
16 Sarén T, Saronio G, Marti Torrell P, *et al*. Complementarity-determining region clustering may cause CAR-T cell dysfunction. *Nat Commun* 2023;14:4732.
17 Long AH, Haso WM, Shern JF, *et al*. 4-1BB costimulation ameliorates T cell exhaustion induced by tonic signaling of chimeric antigen receptors. *Nat Med* 2015;21:581–90.
18 Adachi K, Kano Y, Nagai T, *et al*. IL-7 and CCL19 expression in CAR-T cells improves immune cell infiltration and CAR-T cell survival in the tumor. *Nat Biotechnol* 2018;36:346–51.
19 Lynn RC, Weber EW, Sotillo E, *et al*. c-Jun overexpression in CAR T cells induces exhaustion resistance. *Nature New Biol* 2019;576:293–300.
20 Zhao Y, Chen J, Andreatta M, *et al*. IL-10-expressing CAR T cells resist dysfunction and mediate durable clearance of solid tumors and metastases. *Nat Biotechnol* 2024.
21 Xu Y, Yang Z, Horan LH, *et al*. A novel antibody-TCR (AbTCR) platform combines Fab-based antigen recognition with gamma/delta-TCR signaling to facilitate T-cell cytotoxicity with low cytokine release. *Cell Discov* 2018;4:62.
22 Helsen CW, Hammill JA, Lau VWC, *et al*. The chimeric TAC receptor co-opts the T cell receptor yielding robust anti-tumor activity without toxicity. *Nat Commun* 2018;9:3049.
23 Baeuerle PA, Ding J, Patel E, *et al*. Synthetic TRuC receptors engaging the complete T cell receptor for potent anti-tumor response. *Nat Commun* 2019;10:2087.
24 Liu Y, Liu G, Wang J, *et al*. Chimeric STAR receptors using TCR machinery mediate robust responses against solid tumors. *Sci Transl Med* 2021;13.

25 Mansilla-Soto J, Eyquem J, Haubner S, *et al*. HLA-independent T cell receptors for targeting tumors with low antigen density. *Nat Med* 2022;28:345–52.

26 Cohen CJ, Li YF, El-Gamil M, *et al*. Enhanced antitumor activity of T cells engineered to express T-cell receptors with a second disulfide bond. *Cancer Res* 2007;67:3898–903.

27 Haga-Friedman A, Horovitz-Fried M, Cohen CJ. Incorporation of transmembrane hydrophobic mutations in the TCR enhance its surface expression and T cell functional avidity. *J Immunol* 2012;188:5538–46.

28 Tagod MSO, Mizuta S, Sakai Y, *et al*. Determination of human γδ T cell-mediated cytotoxicity using a non-radioactive assay system. *J Immunol Methods* 2019;466:32–40.

29 Wang Y, Wang L, Seo N, *et al*. CAR-Modified Vγ9Vδ2 T Cells Propagated Using a Novel Bisphosphonate Prodrug for Allogeneic Adoptive Immunotherapy. *IJMS* 2023;24:10873.

30 Ishihara M, Miwa H, Fujiwara H, *et al*. αβ-T cell receptor transduction gives superior mitochondrial function to γδ-T cells with promising persistence. *i Sci* 2023;26:107802.

31 Wherry EJ, Ha S-J, Kaech SM, *et al*. Molecular signature of CD8+ T cell exhaustion during chronic viral infection. *Immunity* 2007;27:670–84.

32 Khan O, Giles JR, McDonald S, *et al*. TOX transcriptionally and epigenetically programs CD8+ T cell exhaustion. *Nature New Biol* 2019;571:211–8.

33 Gumber D, Wang LD. Improving CAR-T immunotherapy: Overcoming the challenges of T cell exhaustion. *EBioMedicine* 2022;77:103941.

34 Selli ME, Landmann JH, Arveseth C, *et al*. Inducing T cell dysfunction by chronic stimulation of CAR-engineered T cells targeting cancer cells in suspension cultures. *STAR Protoc* 2023;4:101954.

35 Garfall AL, Dancy EK, Cohen AD, *et al*. T-cell phenotypes associated with effective CAR T-cell therapy in postinduction vs relapsed multiple myeloma. *Blood Adv* 2019;3:2812–5.

36 Gattinoni L, Klebanoff CA, Palmer DC, *et al*. Acquisition of full effector function in vitro paradoxically impairs the in vivo antitumor efficacy of adoptively transferred CD8+ T cells. *J Clin Invest* 2005;115:1616–26.

37 López-Cantillo G, Urueña C, Camacho BA, *et al*. CAR-T Cell Performance: How to Improve Their Persistence? *Front Immunol* 2022;13:878209.

38 Rafiq S, Hackett CS, Brentjens RJ. Engineering strategies to overcome the current roadblocks in CAR T cell therapy. *Nat Rev Clin Oncol* 2020;17:147–67.

39 Kuwana Y, Asakura Y, Utsunomiya N, *et al*. Expression of chimeric receptor composed of immunoglobulin-derived V regions and T-cell receptor-derived C regions. *Biochem Biophys Res Commun* 1987;149:960–8.

40 Gross G, Waks T, Eshhar Z. Expression of immunoglobulin-T-cell receptor chimeric molecules as functional receptors with antibody-type specificity. *Proc Natl Acad Sci U S A* 1989;86:10024–8.

41 Bos R, Sherman LA. CD4+ T-cell help in the tumor milieu is required for recruitment and cytolytic function of CD8+ T lymphocytes. *Cancer Res* 2010;70:8368–77.

42 Novy P, Quigley M, Huang X, *et al*. CD4 T cells are required for CD8 T cell survival during both primary and memory recall responses. *J Immunol* 2007;179:8243–51.

43 Rodriguez-Marquez P, Calleja-Cervantes ME, Serrano G, *et al*. CAR density influences antitumoral efficacy of BCMA CAR T cells and correlates with clinical outcome. *Sci Adv* 2022;8:eabo0514.

44 Eyquem J, Mansilla-Soto J, Giavridis T, *et al*. Targeting a CAR to the TRAC locus with CRISPR/Cas9 enhances tumour rejection. *Nature New Biol* 2017;543:113–7.

45 Okamoto S, Amaishi Y, Goto Y, *et al*. A Promising Vector for TCR Gene Therapy: Differential Effect of siRNA, 2A Peptide, and Disulfide Bond on the Introduced TCR Expression. *Mol Ther Nucleic Acids* 2012;1:e63.

46 Tokatlian T, Asuelime GE, Naradikian MS, *et al*. Chimeric Antigen Receptors Directed at Mutant KRAS Exhibit an Inverse Relationship Between Functional Potency and Neoantigen Selectivity. *Cancer Res Commun* 2022;2:58–65.

47 Xie G, Ivica NA, Jia B, *et al*. CAR-T cells targeting a nucleophosmin neoepitope exhibit potent specific activity in mouse models of acute myeloid leukaemia. *Nat Biomed Eng* 2021;5:399–413.